Published in final edited form as:
J Membr Biol. 2009 April ; 228(3): 125–140. doi:10.1007/s00232-009-9165-5.

Slc26A9 - anion exchanger, channel and Na^+ transporter

Min-Hwang Chang[1,2,*], **Consuelo Plata**[1,3,*], **Kambiz Zandi-Nejad**[4,*], **Aleksandra Sinđić**[1,2], **Caroline R. Sussman**[1,2], **Adriana Mercado**[4], **Vadjista Broumand**[4], **Viswanathan Raghuram**[5], **David B. Mount**[4,6], and **Michael F. Romero**[1,2,§]

[1]Physiology & Biophysics, Case Western Reserve University, Cleveland, OH 44106

[2]Physiology & Biomedical Engineering, Mayo Clinic College of Medicine, Rochester, MN 55905 USA

[3]Instituto Nacional de Ciencias Médicas y Nutrición, Nefrología y Metabolismo Mineral, México 14000

[4]Renal Div, Brigham & Women's Hospital, Boston, MA, 02115

[5]NHLBI, NIH, Bethesda, MD 20892

[6]Renal Div, VA Boston Healthcare System, W Roxbury MA, 02132

Abstract

The SLC26 gene family encodes anion transporters with diverse functional attributes: (a) anion exchanger, (b) anion sensor and (c) anion conductance (likely channel). We have cloned and studied Slc26a9, a paralog expressed mostly in lung and stomach. Immunohistochemistry shows that Slc26a9 is present at apical and intracellular membranes of lung and stomach epithelia. Using expression in *Xenopus laevis* oocytes and ion-sensitive microelectrodes, we discovered that Slc26a9 has a novel function not found in any other Slc26 proteins – cation coupling. Intracellular pH and voltage measurements show that Slc26a9 is a $n\mathrm{Cl}^-$-$\mathrm{HCO_3}^-$ exchanger, suggesting roles in gastric HCl secretion or pulmonary $\mathrm{HCO_3}^-$ secretion; Na^+ electrodes and uptakes reveal that Slc26a9 has a cation-dependence. Single channel measurements indicate that Slc26a9 displays discrete open and close states. These experiments show that Slc26a9 has three discrete physiological modes: $n\mathrm{Cl}^-$-$\mathrm{HCO_3}^-$ exchanger, Cl^- channel, and Na^+-anion cotransporter. Thus, the Slc26a9 transporter-channel is uniquely suited for dynamic and tissue-specific physiology or regulation in epithelial tissues.

Keywords

intracellular pH; Cl^-; Na^+; $\mathrm{HCO_3}^-$; *Xenopus* oocyte expression; epithelial localization

Introduction

The Slc26 gene family encodes 10 transport proteins with diverse physiology. Slc26a1 (Sat-1) encodes a $\mathrm{SO_4}^{2-}$ transporter shown to exchange $\mathrm{SO_4}^{2-}$ for oxalate (Bissig et al., 1994) and possibly $\mathrm{HCO_3}^-$. Other family members were identified by positional cloning of disease genes: diastrophic dysplasia (SLC26A2/DTDST) (Hastbacka et al., 1992), congenital chloride diarrhea (SLC26A3/DRA) (Hoglund et al., 1996; Schweinfest et al., 1993) and Pendred syndrome (SLC26A4/pendrin) (Everett et al., 1997). Slc26a5 (prestin) was identified as a "molecular motor" of cochlear outer hair cells (Zheng et al., 2000). SLC26A6 was identified

§Address correspondence (current address) to: Michael F. Romero, Ph.D., Dept. Physiology & Biomedical Engineering, Mayo Clinic College of Medicine, 200 First St SW, Rochester, MN 55905; E-mail: romero.michael@mayo.edu.
*contributed equally

as a candidate gene for the apical, exocrine pancreas, HCO_3^- transporter (Lohi et al., 2000) and the proximal tubule Cl^--formate exchanger (Knauf et al., 2001).

Many anions are transported by SLC26 proteins(Bissig et al., 1994; Karniski et al., 1998; Moseley et al., 1999; Mount & Romero, 2004; Satoh et al., 1998; Scott & Karniski, 2000; Soleimani et al., 2001): SO_4^{2-}, Cl^-, I^-, formate$^-$, oxalate^{2-} (ox^{2-}), OH^- and HCO_3^-. Functional characterization of Slc26 proteins has revealed distinctive patterns of anion specificity, *cis*-inhibition, and transport modes. Mouse Slc26a6 transports most of the above substrates (Xie et al., 2002a). In contrast, Slc26a1 transports SO_4^{2-} and ox^{2-} but not Cl^- or formate (Bissig et al., 1994; Karniski et al., 1998; Satoh et al., 1998; Xie et al., 2002a). SLC26A4 transports only monovalent anions but not divalent anions (Scott & Karniski, 2000; Scott et al., 1999).

The physiological role(s) of individual SLC26 anion exchangers is a function of both substrate specificity and tissue expression. As noted, the diverse physiological impact of Slc26 proteins is illustrated by loss-of-function (disease) phenotypes. SLC26A3 is found in colonic epithelial brush border membranes (Haila et al., 2001; Moseley et al., 1999) and helps to mediate colonic, transepithelial salt transport. Its mutation results in severe congenital diarrhea (Hoglund et al., 1996). SLC26A2 mutations cause disordered skeletal development by impairing SO_4^{2-} uptake of chondrocytes and resulting in decreased extracellular matrix sulfation (Hastbacka et al., 1996). This sulfation loss decreases responsiveness to matrix-dependent developmental cues, e.g., FGF.

Novel family members were initially noticed in databases of mammalian expressed sequence tags (ESTs) (Everett & Green, 1999) and some initial characterization was reported (Lohi et al., 2002). Slc26a7 was initially reported to function as a Cl^--HCO_3^- exchanger (Petrovic et al., 2003) and more recently as an anion conductance (Kim et al., 2005). Slc26a9 was reported as a Cl^--HCO_3^- exchanger specific to gastric surface epithelia (Xu et al., 2005), while recent work portrays Slc26a9 as an anion conductance with minimal HCO_3^- transport (Dorwart et al., 2007). Notably, large cellular currents imply “channel activity,” but such currents are not definitive evidence of channel function.

We cloned several of these novel Slc26 members (Xie et al., 2002b) and reported the initial detailed characterization of Slc26a6 as a novel electrogenic Cl^--$n HCO_3^-$ exchanger (Xie et al., 2002a). The present extensive analysis of Slc26a9 reveals that it has physiological activities *not* found together in any other Slc26 proteins: nCl^--HCO_3^- exchanger, Na^+/anion cotransporter and anion channel. Importantly, we provide single channel data and other experiments illustrating a Na^+-coupled transport mode. Slc26a9 is the first, and perhaps only, Slc26 member to show Na^+ (cation) coupling. We hypothesize that these diverse activities allow Slc26a9 to fulfill a wide variety of physiological roles in the lung and stomach, and likely allow quick, dynamic physiological regulation in these tissues.

Methods

Cloning of SLC26A9 and Slc26a9

Human SLC26A9 exons were identified in BAC clone sequences (RP11-196022, RP11-370I5). 3′ SLC26A9 genomic sequences were used to search for human 3′-UTR ESTs. The identified IMAGE clone 2915384 was obtained and sequenced (bp 2502 - 4526 of the final cDNA). The open reading frame was then cloned by RT-PCR of human lung with Takara LaPCR polymerase with specific primers (Table 1). PCR fragments were subcloned into pCR2.1 (Invitrogen) and sequenced. A 500,000 bp contig containing the entire mouse Slc26a9 gene was identified by a *blastn* search of the Celera mouse genomic database with human SLC26A9 (*AF314958*). The Slc26a9 cDNA (3049 bp; *AY034145*) was amplified by RT-PCR

from mouse lung with a mouse primers (Table 1) and subcloned into the *Xenopus laevis* expression vector pGEMHE.

Localization of Slc26a9 mRNA

Northern analysis—RNA was extracted from mice using guanidine isothiocyanate and CsCl. Total RNA (10 μg/lane) was size-fractionated by electrophoresis (5% formaldehyde, 1% agarose), transferred to a nylon membrane (Stratagene), and probed with ^{32}P-labeled randomly-primed (DecaPrime, Ambion) gene-specific probes for Slc26a9 and full-length GAPDH. The Slc26a9 probe was generated by PCR (bp 2203-2810), as were the probes for human SLC26A9 (bp 291-822) and SLC26A6 (2090 to 2587). Hybridization was overnight at 42°C (4X SSCP/40% formamide/4X Denhart's solution/0.5% SDS/200 μg salmon sperm DNA) and membranes were washed twice for 10 min at room temperature in 2X SSCP/0.1% SDS, and twice for 1 hr at 65C in 0.1X SSCP/0.1% SDS.

RT-PCR—Total RNA (200 ng/reaction) from mouse tissues was reverse transcribed using oligo(dT) priming. PCR amplification was performed as described (Mount et al., 1999), using Taq-2000 polymerase (Stratagene). The Slc26a9 primers (Table 1) amplified a 354 bp band. RT-PCR with a GAPDH-specific primer pair (Table 1) amplified a 571 bp band

Protein Localization

Slc26a9 antibodies—To localize mSlc26a9, we generated two rabbit peptide antibodies against the C-terminus: "CQEL" (C-QELQQDFESAPSTDPNN) and "aCKQ" (acetyl-C-KQKYLRKQEKRTAIPTQQRK) (Quality Control Biochemicals, Hopkinton, MA). "ACKQ" had superior reactivity and was used for all experiments reported (now referred to as "Slc26a9 antibody"). We verified Slc26a9 antibody specificity by Western analysis of oocytes expressing Slc26 protein, as previously performed for other transporters (Schmitt et al., 1999; Sciortino et al., 2001). The Slc26a9 antibody recognized the appropriate size protein in Slc26a9 oocytes but not water-injected controls or cells expressing other SLC26 transporters (See Fig 2A).

Immunohistochemistry—Mice were perfusion fixed with PBS followed by 4% paraformaldehyde-lysine-periodate (PLP) (Schmitt et al., 1999). Tissues were dissected and fixed several hrs in PLP followed by overnight 30% sucrose in PBS at 4°C (Sciortino et al., 2001). OCT (cryomedia) embedded tissue was cryosectioned at 10 μm. Immunostaining was performed using 1:100 dilution of the primary Slc26a9 antibody and a Cy3 secondary antibody. Epifluorescent images were captured using a Zeiss AxioVert 25 microscope (Dinour et al., 2004; Sciortino et al., 2001).

Oocyte experiments

Female *X. laevis* were purchased from Xenopus Express (Beverly Hills, FL). Slc26 clones were subcloned into the pGEMHE *Xenopus* expression vector (Liman, Tytgat & Hess, 1992). Oocytes were collagenase dissociated (Romero et al., 1998). Capped cRNA was synthesized using the T7 mMessage mMachine kit (Ambion, Austin, TX). Oocytes were injected with 50 nL cRNA (0.5 μg/μL, 25 ng/oocyte) or water, and incubated at 16°C in OR_3 media, unless otherwise indicated. Oocytes were studied 3-10 days after injection.

Uptake experiments—$^{36}Cl^-$ and $^{22}Na^+$ uptakes were performed as previously (Plata et al., 2007; Xie et al., 2002a). Briefly, oocytes were pre-incubated for 20 min in $0Cl^-$ and $0Na^+$ uptake medium (in mM: 100 NMDG-gluconate, 2 K-gluconate, 1 Ca-gluconate, 1 Mg-gluconate, 10 HEPES-Tris, pH 7.5). Oocytes were then incubated for 60 min with isotope. Cells were washed 3x in uptake buffer with 5 mM cold uptake buffer. Oocytes were

individually dissolved in 10% SDS and tracer activity determined by scintillation counting. Cl^- uptake was performed using the same $0Cl^-$ uptake solution (8.3 mM $^{36}Cl^-$). For Na^+ experiments, we added 100 mM Na^+ to replace 100 mM NMDG and included furosemide (100 μM) to inhibit the oocyte Na^+-K^+-$2Cl^-$ cotransporter. The uptake experiments included 12-18 oocytes in each experimental group (mean±SEM). Statistical significance was $p<0.05$ using a two-tailed Student's t-test.

Electrophysiology—All solutions were either ND96 (96 mM NaCl, 2 mM KCl, 1.8 mM $CaCl_2$, 1 mM $MgCl_2$, 5 mM HEPES, pH 7.5) or iso-osmotic ion replacements (Sciortino & Romero, 1999). The Na^+ replacement was NMDG; and the Cl^- replacement was gluconate. For HCO_3^- solutions, we used 5% CO_2/ 33 mM HCO_3^- (pH 7.5).

Two electrode voltage clamp

For these experiments, oocytes were injected with 0.5 ng cRNA and membrane currents were recorded with an OC-725C voltage clamp (Warner Instruments, Hamden, CT), filtered at 2-5 kHz, digitized at 10 kHz. I-V protocols consisted of 40 ms steps from V_h (-60 mV) to −160 mV and +60 mV in 20 mV steps (Dinour et al., 2004; Sciortino & Romero, 1999).

Ion selective microelectrodes

Ion selective microelectrodes were used to monitor pH_i, Cl^- ($[Cl^-]_i$) and intracellular Na^+ activity ($[Na^+]_i$) of oocytes (Romero et al., 1998; Romero et al., 2000; Sciortino & Romero, 1999). Intracellular pH, Cl^- and Na^+ microelectrodes had slopes of at least -54 mV/pH unit or decade, respectively.

Patch clamp and Single-Channel Analysis—Most patch-clamp recordings were performed in excised inside-out patches of CHO cells (similar results were obtained with Slc26a9-oocytes or transfected HEK cells). Patch pipettes were 10-20 MΩ; membrane seals were >10 GΩ. The bath and pipette solutions contained (in mM) 138 NMDG-Cl, 2 $MgCl_2$, and 10 HEPES (pH 7.5). All experiments were performed at room temperature. Single-channel currents were amplified using an Axopatch-200B amplifier (Axon Instruments, Foster City, CA.), filtered at 100 Hz, and computer transferred via an ITC-18 interface (Instrutech Corp, Port Washington, NY). Data were digitized at 2 kHz and written directly on to hard disk using Pulse 8.65 (HEKA, Lambrecht, Germany) software. The applied potential is the pipette electrode potential minus the bath electrode reference potential (+ current: pipette to bath). Current records were analyzed by TAC software (Bruxton, Seattle, WA) and plotted using IgorPro (WaveMetrics, Lake Oswego, OR).

Results

Slc26a9 expression and chromosomal localization

A 5 kb Slc26a9 transcript is found in lung and stomach of mouse and human (not shown). Both mouse Slc26a9 and human SLC26A9 have a predicted C-terminal type-I PDZ interaction motif (SEV) (see *Discussion*).

Radiation hybrid mapping places human *SLC26A9* at chromosome 1q31-32. Murine *Slc26a9* is physically linked on Celera contigs to STS markers and genes (*cathepsin E*, *Mdm4*, *ELK4*, and *PCTK3*) located on the syntenic region of murine chromosome 1 at ~70 cM (Mouse Genome Database).

RT-PCR showed that Slc26a9 is in lung and stomach and detectable in brain, heart, kidney, thymus, spleen and ovary (Fig 1)

Protein localization

To determine Slc26a9 cellular localization, we generated a rabbit polyclonal, C-terminal-peptide antibody. The Slc26a9 antibody specificity was determined by assessing cross-reactivity with other recombinant Slc26 proteins expressed in oocytes (Fig 2A). The Slc26a9 antibody recognizes a protein of ~87 kDa only from oocytes injected with Slc26a9 cRNA.

Next, we examined the tissue Slc26a9 localization in mouse lung (Fig 2B) and stomach (Fig 2C&D). Staining is apparent in both bronchial epithelia and alveolar cells. The Slc26a9 blocking peptide (BP) eliminated lung staining (Fig 2B, right panels).

Using an antibody to H^+/K^+-ATPase, we colocalized Slc26a9 with this marker of gastric crypt epithelia. Slc26a9 is found at the apical membrane of gastric surface epithelia and intracellular membranes (Fig 2C&D) as reported by Xu (Xu et al., 2005). The Slc26a9 protein is also immunolocalized to apical membranes of gastric gland crypt epithelia (Fig 2D). The stomach staining is eliminated by the Slc26a9-blocking peptide (Fig 2C, right panels). Thus, Slc26a9 is highly expressed in both the less differentiated epithelial population (surface) and the terminally differentiated epithelia (crypt). Modest, yet obvious, Slc26a9 staining occurs in cells expressing the H^+/K^+-ATPase. Higher magnification evaluation of these H^+/K^+-ATPase positive cells reveals some overlapping and some adjacent Slc26a9 staining (not shown).

HCO_3^- transport

To determine if Slc26a9 functions as a Cl^--HCO_3^- exchanger, we measured intracellular pH (pH_i) changes after Cl^- removal and re-addition from the CO_2/HCO_3^- bath solution. Since we and others have found that some Slc26 transporters are electrogenic (Ko et al., 2002; Xie et al., 2002a), we also measured V_m changes simultaneously. Water-injected oocytes exposed to bath CO_2/HCO_3^- acidified quickly (Fig 3A, D). These and our previous results showed that Na^+ and Cl^- dependent HCO_3^- transport is absent from water-injected-oocytes (Romero et al., 1997; Romero et al., 2000; Xie et al., 2002a). The initial pH_i is similar for water control- and Slc26a9- or Slc26a7-expressed oocytes. Bath CO_2/HCO_3^- addition decreases pH_i of Slc26a9 injected oocytes (Fig 3B, E) similar to water control oocytes. HCO_3^- addition also causes a small depolarization in Slc26a9-injected oocytes (Fig 3E), reminiscent of the anion conductance observed with NDAE1 (Romero et al., 2000) and Slc26a6 (Xie et al., 2002a). In water controls, Cl^- replacement (with gluconate, "$0Cl^-$") did not change pH_i or V_m. On the other hand, for Slc26a9, $0Cl^-$ increases pH_i (alkalinization) which stops with Cl^- re-addition. $0Cl^-$ also evokes a depolarization in Slc26a9-injected oocytes (Fig 3E). By contrast, $0Cl^-$ hyperpolarized the Slc26a6-oocytes (Xie et al., 2002a). For Slc26a7-oocytes, $0Cl^-$ depolarized the oocyte but did not increase pH_i (Fig 3C) as observed with either Slc26a6 or Slc26a9. The rate of pH_i change (Fig 3D) and V_m changes (Fig 3E) associated with Cl^- removal were repeated for the second time after the readdition of Cl^-. For Slc26a9, $0Cl^-$ (in O_2 bubbled solutions; initial part of Fig 3B) gave similar results ($\uparrow pH_i$, $+27 \pm 4.6\times10^{-5}$ pH units/s; ΔV_m, $+114\pm7.0$ mV, n=5). Thus, Slc26a9 has a *n*Cl^--OH^- exchange mode.

Acid-base transport via Slc26a9 is further evidenced by a pH_i overshoot. This overshoot is due to HCO_3^- loading of the oocyte due to prolonged exposure to CO_2/HCO_3^-. Prior to CO_2 removal, pH_i rose to 7.1 (Fig 3B). CO_2/HCO_3^- removal elicited a robust alkalinization and pH_i overshoot to 7.7 (7.79 ± 0.11, n=7), i.e., cell HCO_3^- loading ($+0.37 \pm0.06$ pH units > starting pH_i) (Romero et al., 1998;Romero et al., 2000). This overshoot is not observed in controls (Fig 3A) or Slc26a7-oocytes (Fig 3C). The Slc26a9 oocytes also showed a hyperpolarization (~5-7 mV) with CO_2/HCO_3^- removal.

Other than a dependence on bath pH, no Slc26 proteins have been shown to participate in cation transport. To test a potential role of Na^+ in Slc26a9-mediated transport, we replaced Na^+ with

NMDG in CO_2/HCO_3^- solutions. Sodium removal depolarizes Slc26a9-oocytes (Fig 3E) and pH_i is also reduced (Fig 3B; dpH_i/dt in Fig 3D). This depolarization and acidification is similar to a "low activity" electrogenic $Na^+/nHCO_3^-$ cotransporter (Romero et al., 1997), an activity not observed in control oocytes (Fig 3A; dpH_i/dt in Fig 3D; ΔV_m in Fig 3E).

Cl^- transport

The large depolarization resulting from $0Cl^-$ (HCO_3^- solution) implied that multiple intracellular Cl^- ions are exchanged for each extracellular HCO_3^- ($\underline{n}Cl^-:1HCO_3^-$). To directly examine Cl^- transport by Slc26a9, we measured intracellular Cl^- concentration ($[Cl^-]_i$) and V_m simultaneously (Fig 4). Resting $[Cl^-]_i$ in Slc26a9 expressed oocytes was lower than water injected control oocytes (29.3±2.8 mM; n=21 vs. 39.4±2.7 mM; n=14, respectively). Unlike the control oocyte (Fig 4A), Cl^- removal causes a vigorous $[Cl^-]_i$ decrease (Cl^- efflux) in the Slc26a9 oocyte (Fig 4B). $0Cl^-$ elicited an rapid Cl^- drop (-5.1 mM Cl^-/min) such that in 5 min $[Cl^-]_i$ had fallen by 12-19 mM with a 60 mV depolarization. This dramatic $[Cl^-]_i$ fall was not observed in control oocytes (-0.62 mM Cl^-/min; Fig 4A). Bath Cl^- re-addition neither increased nor returned $[Cl^-]_i$ to initial levels (Fig 4B), indicating that Cl^- efflux is Slc26a9's dominant mode.

Na^+ transport

Based on our pH_i experimental results (Fig 3A, B), we sought to determine if Na^+ altered Slc26a9-mediated transport. Specifically, does Slc26a9 transport Na^+?

Using Na^+ selective microelectrodes and ^{22}Na, we measured intracellular $[Na^+]$ ($[Na^+]_i$) changes and Na uptake in Slc26a9- and water-injected oocytes (Fig 5). Resting $[Na^+]_i$ was similar in both water controls (Fig 5A) and Slc26a9 expressing oocytes (Fig 5B). $0Na^+$ caused a $[Na^+]_i$ decrease (Na^+ efflux; -0.48±0.16 mM, n=8) and a depolarization (+6.8±0.7 mV, n=8) in Slc26a9 oocytes (electrogenic $Na^+/\underline{n}$Anion cotransport) but not in controls (-6.6±1.1 mV, n=7). Simultaneous Cl^- removal ($0Na^+$-$0Cl^-$) resulted in a further $[Na^+]_i$ decrease (Fig 5B; -0.71±0.23 mM, n=8) and robust depolarization (>60 mV). Na^+ readdition raise $[Na^+]_i$ in Slc26a9 oocytes (+1.31±0.24 mM, n=8), and sequential Cl^- readdition further increased $[Na^+]_i$ (+1.23±0.18 mM, n=8). $0Cl^-$ alone reversibly decreased $[Na^+]_i$ in Slc26a9 but not in control oocytes. Fig 5C shows that Slc26a9-oocytes but not Slc26a6-oocytes have a higher ^{22}Na uptake than water injected control oocytes. This Na^+ transport is reversible indicating that Slc26a9 participates in both Na^+ efflux (measured by electrodes) and Na^+ influx (measured by both electrodes and ^{22}Na). The conclusion on Na^+ transport by Slc26a9 is further strengthened by the result in Fig 5D showing that $^{36}Cl^-$ uptake by Slc26a9 was increased by the presence of extracellular Na^+ (500 pmole/oocyte/hr).

Current-voltage (I-V) relationships

We previously reported large currents with Slc26a9 activity (Romero et al., 2006). Another report found similar activity (Dorwart et al., 2007) and examined the halide selectivity of human SLC26A9. With 25 ng of Slc26a9-cRNA, we could easily measure the "transporter" modes of Slc26a9. However, this amount of cRNA resulted in currents beyond the capabilities of our voltage clamp. Thus for voltage clamp experiments, we used 0.5 ng/oocyte injections.

We tested the Cl^- and cation dependence of these currents (Slc26a9, Fig 6A-C; control, Fig 6D-F). In $0Cl^-$, oocyte currents are modest (Fig 6A) but still larger than controls. Cl^- addition greatly increased Slc26a9 currents (>20 μA, Fig 6B). Microelectrodes experiments measuring a huge intracellular $[Cl^-]$ drop after Cl^- removal (Fig 4B) also implicated Cl^- as the current charge carrier. Sodium removal ($0Na^+$) decreased the current magnitude which suggested again the Na^+-coupling of Slc26a9 transport $0Na^+$ minimized a time dependent current (after 10 ms),

but not the initial step currents (Fig 6C). None of these Slc26a9-currents were observed in the water-control oocytes (Fig 6D-F).

Anion conductance

To determine if the large currents found in Slc26a9 were a "pure" Cl^- conductance (e.g., Cl^- channel), we varied the extracellular $[Cl^-]$ ($[Cl^-]_o$) while measuring $[Cl^-]_i$ and V_m (Fig 7A). These experiments allowed us to compare the $[Cl^-]_i$ change in response to $[Cl^-]_o$ changes. There is a linear relationship between the equilibrium potential (E_{Cl}) and $[Cl^-]_o$ (15-104 mM). We also obtained IV curves while varying bath Cl^- (Fig 7B, left). These data show that the I_{max}^{Cl-} occurs when $[Cl^-]$ is >104 mM (Fig 7B, right). Next, we tested for asymmetric "channel gating," i.e., can Slc26a9 Cl^- currents be activated or inactivated with a voltage pre-pulse (Fig 7C: +60 mV, blue; resting V_m, black; -140 mV, red). These experiments illustrate the Slc26a9-IV relationships are not pre-pulse dependent and that there is no "inactivation" state as predicted in many channel kinetic schemes.

Patch recordings

0.5 ng injections of Slc26a9 cRNA lead to tens of μA currents (Fig 6), and Slc26a9 oocytes act as an almost perfect Cl^- electrode (Fig 7A). Therefore, we used inside-out excised patch clamp experiments to determine if Slc26a9 expression (oocytes, HEK cells, and CHO cells) resulted in single channel events (Fig 8).

Fig 8A shows obvious single channel events from one such patch (CHO cells). In symmetric NaCl solutions, holding at -100 mV resulted in a ~3.2 pS channel conductance. The Slc26a9 channel response to different holding potentials is shown in Fig 8B. Similar channel activity was evident in oocytes and HEK cells (not shown). These single channel events were not observed in non-transfected CHO control cells (Fig 8C).

Discussion

The Slc26 protein family encodes diverse anion transporters which when mutated cause a variety of human diseases: diarrhea, deafness, goiter, diastrophic dysplasia, etc. Within this novel anion transporter group, the Slc26a9 protein displays further surprising functions, e.g., $n Cl^-$-HCO_3^- exchange, single Cl^- channels and Na^+-coupling. Comparative genomic analysis indicates that the Slc26a9 gene may have arisen as recently as the emergence of amphibians but at least after teleosts (Romero, personal observation, see below).

Slc26a9 (electrogenic $n Cl^-$-HCO_3^- exchanger and Cl^- channel) branches with Slc26a5 (prestin, anion receptor) and Slc26a6 (electrogenic Cl^--$n HCO_3^-$ exchanger) in the Slc26 family. Yet, Slc26a7 (apparent Cl^- channel conductance) is found in a different branch of the Slc26 family. "How" these disparate transport functions arose will require a more detailed knowledge of the molecular determinants of anion recognition and transport.

Our uptake data for mouse Slc26a9 differ from that published for human SLC26A9 (Lohi et al., 2002). Lohi et al reported that SLC26A9-injected cells mediate uptake of SO_4^{2-}, Cl^-, oxalate (ox^{2-}) and formate (Lohi et al., 2002). Perhaps some differences are due to species variation, although mouse and human Slc26a9 are ~90% identical. Notably, the reported cis-inhibition data lack a positive-control (e.g. Slc26a6) for the substrates tested. These cis-inhibition data also disagree with uptake measurements in the same study (Lohi et al., 2002), i.e., oxalate was a substrate but did not cis-inhibit $^{35}SO_4^{2-}$ uptake.

Similar discrepancies exist in the reported transport characteristics of other Slc26 paralogs. Several groups have reported that SLC26A3 transports SO_4^{2-}. Our data (Romero et al., 2006) and those of Chernova (Chernova et al., 2003) indicate that SO_4^{2-} is not a human SLC26A3

substrate. Of note, we (Romero et al., 2006) and Chernova found $^{36}Cl^-$ uptakes for Slc26a3 (Chernova et al., 2003) of 20- to 40-fold greater than our water controls, versus Moseley's one-fold greater than controls (Moseley et al., 1999), the first report of SLC26A3 SO_4^{2-} transport. Consistent with Scott and Karniski's data, SLC26A4, the closest human SLC26A3 paralog, is specific for monovalent anions and does not transport SO_4^{2-} (Scott & Karniski, 2000; Scott et al., 1999).

As with Slc26a6 (Xie et al., 2002a), we determined whether Slc26a9 was capable of Cl^--HCO_3^- exchange and what the nature of this exchange might be. ΔpH_i measurements elicited by the extracellular $0Cl^-$ ($^+HCO_3^-$) shows that Slc26a9 functions as a nCl^--HCO_3^- exchanger (Fig 3B). This same type of experiment showed that Slc26a6 was an electrogenic Cl^--$nHCO_3^-$ exchanger (Xie et al., 2002a). Slc26a7 (in an oocyte expression vector) had no obvious Cl^--HCO_3^- exchange (see *Results*, Fig 3C) as previously suggested (Petrovic et al., 2003). Collectively, these Slc26 transporters (a3, a4, a6, a9) represent novel physiological activities - electrogenic Cl^--HCO_3^- exchange - not anticipated by prior animal or tissue physiology studies (Ko et al., 2002; Xie et al., 2002a).

Our Slc26a9 characterization adds to the novel activities mediated by these Slc26 proteins. Cl^- removal evokes a significant depolarization and pH_i increase (HCO_3^- uptake). These Slc26a9 results differ from Slc26a6-injected oocyte data for which $0Cl^-$ causes a strong *hyperpolarization* (Kato et al., 2008; Ko et al., 2002; Kurita et al., 2008; Shcheynikov et al., 2006; Xie et al., 2002a). The data presented here are, however, consistent with either cation-coupled HCO_3^- exchange for Cl^- (Na^+ driven Cl^--HCO_3^- exchange) or exchange of $\underline{n}Cl^-$ for 1 HCO_3^- (electrogenic nCl^--HCO_3^-).

Slc26a9 is the first Slc26 member with cation-coupling. Specifically, Na^+ replacement by choline decreases pH_i and depolarizes Slc26a9-expressing oocytes (Fig 3B) or reduces whole cell currents (Fig 6C). This novel aspect of Slc26a9 transport is similar to that of NBCe1 (Romero et al., 1998), i.e., electrogenic Na^+-coupled $nHCO_3^-$ cotransport. While there is both Na^+ and Cl^- dependence of transport, these modes do not appear interconnected with HCO_3^-. That is, Slc26a9 does not appear to be a different variety of Na^+-driven Cl^--HCO_3^- exchanger (Grichtchenko et al., 2001;Romero et al., 2000). Rather Slc26a9 apparently has two, non-interdependent transporter modes illustrated by (a) $[Na^+]_i$ changing with bath Cl^- removal (Fig 5) yet (b) $[Cl^-]_i$ not changing with bath Na^+ removal (Fig 4). In our hands, Slc26a9 is unique in showing activation of Cl^- uptake at extracellular pH 6 (Romero et al., 2006). We hypothesize that the "pH dependence" observed with other Slc26 proteins (Xie et al., 2002a), may be modified to be a transport site in Slc26a9 as Slc26a9 is likely the most recent addition to the *Slc26* genes.

Several lines of evidence indicate that the presence of cations influence Slc26a9-mediated transport. First, most of the Cl^- uptake experiments were performed under nominally Na^+-free conditions. When extracellular Na^+ is added to the uptake solution Cl^- uptake by Slc26a9 is enhanced (Fig 5D). Second, there is a large Na^+ dependent conductance of Slc26a9 that is also time-dependent (Fig 6). Third, Slc26a9 activity is increased by lowering extracellular pH as we reported previously (Romero et al., 2006). This extracellular pH dependence is **a** 25-fold $[H^+]$ increase (~0.04 μM → 1.00 μM). Thus, this concentration change is a significant "cation-coupling" mode of Slc26a9. Forth, Xu et al found that Slc26a9-mediated Cl^--HCO_3^- exchange was suppressed by NH_4^+ (Xu et al., 2005). Since NH_4^+ is often a K^+ surrogate, it is unlike to act as an interfering cation of the Slc26a9 transporter-channel. Instead, the V_m change typically associated with high $[NH_4^+]$ (or high $[K^+]$) likely alters the Slc26a9-Cl^--HCO_3^- exchange activity since Slc26a9 is controlled by both concentration and electrical driving forces. Together, these data demonstrate a clear cation-coupling mode of Slc26a9.

Slc26a9 expression is highest in lung and stomach (Fig 1). These epithelial cells have prominent CFTR expression and seem to play a major role in pulmonary fluid, Cl^- and HCO_3^- excretion (Ballard et al., 1999). Several reports indicate Cl^--HCO_3^- exchange regulation by CFTR (Choi et al., 2001;Greeley et al., 2001;Wheat et al., 2000). CFTR can also alter the function of Slc26a3, -a4 and -a6 (Ko et al., 2004). Transfecting CFT-1 tracheal epithelial cells (homozygous Δ508-CFTR) with wild-type CFTR results in a stimulation of Cl^--HCO_3^- exchange and SLC26A3 mRNA induction (Wheat et al., 2000). There is a correlation between CFTR mutants, Cl^--HCO_3^- exchange and CF phenotype. Pancreatic insufficiency mutants do not promote cAMP-dependent Cl^--HCO_3^- exchange, yet this regulation is preserved in pancreatic sufficiency mutants (Choi et al., 2001). This is of particular importance since Slc26a9 mediates *n*Cl^--HCO_3^- exchange (Fig 3). Moreover, the Slc26a9 Na^+ coupling may provide a "fail-safe" for gastric epithelia in anion or HCO_3^- absorption (Fig 9), i.e., anion absorption without H^+ absorption or HCO_3^- secretion. This hypothesis of Slc26a9's role in stomach epithelial physiology is further supported by a recent report of a Slc26a9 knockout mouse (Xu et al., 2008). Slc26a9 -/- mice have extensive stomach pathology and a defect in gastric acid secretion. Interestingly, the defect in parietal cell acid secretion implies that Slc26a9 function in the H^+/K^+ pump positive cells (lower Slc26a9 protein in Fig 2C & 2D) is rate limiting for function. These data in light of the Slc26a9 knockout mouse also illustrate that Slc26a9 contributes to functional HCl secretion and that complete protein overlap is not necessary.

Ko and coworkers demonstrated a mutually, stimulatory interaction between the CFTR R-domain and the STAS domains of Slc26a3 and Slc26a6 (Ko et al., 2004). A type I PDZ motif in Slc26a9 suggests that it may "collaborate" with CFTR and other transporters at apical membranes of pulmonary epithelia (Ahn et al., 2001; Wang et al., 2000) or other tissues where Slc26a9 is found (Fig 1D). This would be consistent with our protein localization shown in Fig 2. Again, this localization is supported by the loss of cells in the Slc26a9 -/- mouse (Xu et al., 2008).

There is significant overlap in Slc26 mRNA expression in certain tissues (intestine and secretory epithelia), indicative of physiological redundancy. For example, SLC26A6 is co-expressed with SLC26A9 in Calu-3 cells (Mount and Romero, unpublished observations), suggesting that both play a role in pulmonary HCO_3^- secretion. SLC26A3 and SLC26A6 (Greeley et al., 2001; Lohi et al., 2000) and SLC26A2 (Haila et al., 2001) are expressed apically in pancreatic ductal epithelia. SLC26A2 and SLC26A3 are co-expressed apically in colonic epithelia (Haila et al., 2001; Haila et al., 2000). This co-expression of SLC26 anion exchangers with overlapping transport functions likely has significant genetic and physiological consequences (Fig 9). Key unresolved questions include the specific roles of individual paralogs in specific membranes of specific cell types, e.g. apical membranes of pulmonary epithelial cells, and the degree to which SLC26 paralogs are interdependent or dependent on CFTR transport and regulation.

The electrophysiology experiments here reveal that Slc26a9 has three major ion transport modes: electrogenic *n*Cl^--HCO_3^- exchange, electrogenic $Na^+/\underline{n}Anion^-$ cotransport and anion channel. Recently, the groups of Miller, Jentsch and Pusch have provided compelling evidence that the distinction between channel and transporter is not as definitive as textbooks indicate (Accardi & Miller, 2004; Picollo & Pusch, 2005; Scheel et al., 2005). Likewise, our channel data (Fig 8) and recent Slc26a9 cell conductance data (Dorwart et al., 2007) further blur the accepted distinctions of channels and transporters. Novel to Slc26a9 is that all three modalities are manifested by one protein, versus the functional separation in the CLC family, some paralogs having only Cl^--H^+ exchange and others displaying only channel activity.

The Slc26 gene family has a particular predilection for human genetic disease (Everett & Green, 1999). The newer family members include positional and functional candidates for genetic disorders. SLC26A9 is a positional candidate for pseudohypoaldosteronism type II (Gordon's syndrome), an autosomal hypertensive disorder with linkage to chromosome 1 (Mansfield et al., 1997). Renal expression of SLC26A9 is not observed on Northern blots. However, Slc26a9 can be amplified by RT-PCR from mouse (Fig 1D) and human kidney RNA (not shown), suggesting a role in renal NaCl absorption. SLC26A9 also seems regulated by the WNK1 and WNK4 kinases (Dorwart et al., 2007), the two known genes for pseudohypoaldosteronism type II.

Slc26a9 seems to be a recent addition to the *Slc26* genes, arising at least in amphibians since the *Slc26a9* gene is not found in teleosts such as zebrafish and fugu (Romero, personal observations). *Slc26a9* seems coincident with the emergence of air breathing. Species which are intermediate to amphibians and teleosts (boney fish, Class *Actinopterygii*), such as lung-fish (*Dipnoi* which includes coelacanths) use a modified swim bladder or intestine to absorb O_2 (Bourbon & Chailley-Heu, 2001; DeLaney et al., 1983). This connection may have lead to Slc26a9 mRNA / protein expression in *Tetrapoda* being highest in lung and stomach. In the mudskipper (genus *Periophthalmus*) and weatherloach (*Misgurnus anguillicaudatus*), the transition from water extraction of O_2 to "air-breathing" arises manifesting as intestinal extraction of O_2 from air and thereby allowing aestivation (Ip, Chew & Randall, 2004). Given the prominence of Slc26a9 mRNA in both lung and stomach, this evolutionary connection may associate Slc26a9 with development of "air-breathing." Or, perhaps the novel transport features of Slc26a9 in the stomach and lung are due to selective pressures of terrestrial life or air breathing.

In conclusion, Slc26a9 is a widely expressed Slc26 paralog, particularly abundant in lung and stomach. Slc26a9 moves inorganic ions by three distinct modes: (a) electrogenic $n{Cl^-}$-HCO_3^- exchange, (b) electrogenic Na^+/nAnion cotransport and (c) anion channel. Since many epithelial tissues have traces of Slc26a9 mRNA, discerning Slc26a9 functional roles in these tissues will be important and challenging. Redundancy or overlap of Slc26 protein expression complicates the physiological and structural contributions of this versatile protein family. Since the Slc26a3 and Slc26a6 STAS domains interact with CFTR (Ko et al., 2004) and PDZ-binding sites on Slc26 proteins, specific structures and protein-interactions play a major role for this family (Fig 9). The dynamics of these structural interactions are presently unknown. It is unlikely that these three distint modes of Slc26a9 transport (electrogenic $n{Cl^-}$-HCO_3^- exchanger, Fig 9A; Cl^- channel, Fig 9B; and Na^+/nAnion$^-$ cotransporter, Fig 9C) are simultaneously functioning or even ever functioning in a given cell-type. Accordingly, it is attractive to speculate that kinases/phosphatases, binding proteins and domain structures may dictate the Slc26a9 physiology in specific tissues, e.g., channel (Fig 9B) vs. transporter (Fig 9A and C). For example, given deficit in parietal cell H^+ secretion in the Slc26a9 knockout mouse (Xu et al., 2008), we would expect that either the Cl^- channel mode (Fig 9B) or the electrogenic $n{Cl^-}$-HCO_3^- exchanger mode (Fig 9A) of Slc26a9 is missing in these mice. In other tissues where Slc26a9 expression is more limited (e.g., the kidney), there may be a physiologic need for a dynamic "switching" between these physiological modes to accommodate blood or intracellular signaling. Understanding these diverse functions and their potential regulation will help elucidate the role of SLC26A9 (human) in cystic fibrosis, defects in gastric acid secretion, pseudohypoaldosteronism type II and other epithelial transport pathologies.

Acknowledgments

We thank N Angle, G Babcock, L Song, Q Xie, R Welch, and M Sanders for excellent technical support. We thank Dr. S Muallem for the Slc26a7 cDNA. We also thank Drs. SW Jones and C Objero-Paz for discussions and initial patch experiments.

This work was supported by NIH grants DK056218, DK060845, EY017732 (MFR); DK038226, DK070756, DK57708 (DBM); F32-DK65482 (VB). Other funding includes an Advanced Career Development Award from the Veterans Administration (DBM); Wadsworth Foundation & American Heart Association (CRS); postdoctoral fellowship from AHA (M-HC and KZ); and the Cystic Fibrosis Foundation (ROMERO-06GO and SINDIC-06F0).

References

Accardi A, Miller C. Secondary active transport mediated by a prokaryotic homologue of ClC Cl- channels. Nature 2004;427:803–7. [PubMed: 14985752]

Ahn W, Kim KH, Lee JA, Kim JY, Choi JY, Moe OW, Milgram SL, Muallem S, Lee MG. Regulatory interaction between the cystic fibrosis transmembrane conductance regulator and HCO3- salvage mechanisms in model systems and the mouse pancreatic duct. J Biol Chem 2001;276:17236–43. [PubMed: 11278980]

Ballard ST, Trout L, Bebok Z, Sorscher EJ, Crews A. CFTR involvement in chloride, bicarbonate, and liquid secretion by airway submucosal glands. Am J Physiol 1999;277:L694–9. [PubMed: 10516209]

Bissig M, Hagenbuch B, Stieger B, Koller T, Meier PJ. Functional expression cloning of the canalicular sulfate transport system of rat hepatocytes. J Biol Chem 1994;269:3017–21. [PubMed: 8300633]

Bourbon JR, Chailley-Heu B. Surfactant proteins in the digestive tract, mesentery, and other organs: evolutionary significance. Comp Biochem Physiol A Mol Integr Physiol 2001;129:151–61. [PubMed: 11369540]

Chernova MN, Jiang L, Shmukler BE, Schweinfest CW, Blanco P, Freedman SD, Stewart AK, Alper SL. Acute regulation of the SLC26A3 congenital chloride diarrhoea anion exchanger (DRA) expressed in Xenopus oocytes. J Physiol 2003;549:3–19. [PubMed: 12651923]

Choi JY, Muallem D, Kiselyov K, Lee MG, Thomas PJ, Muallem S. Aberrant CFTR-dependent HCO-3 transport in mutations associated with cystic fibrosis. Nature 2001;410:94–97. [PubMed: 11242048]

DeLaney RG, Laurent P, Galante R, Pack AI, Fishman AP. Pulmonary mechanoreceptors in the dipnoi lungfish Protopterus and Lepidosiren. Am J Physiol 1983;244:R418–28. [PubMed: 6402942]

Dinour D, Chang M-H, Satoh J-I, Smith BL, Angle N, Knecht A, Serban I, Holtzman EJ, Romero MF. A novel missense mutation in the sodium bicarbonate cotransporter (NBCe1/SLC4A4) causes proximal tubular acidosis and glaucoma through ion transport defects. J Biol Chem 2004;279:52238–46. [PubMed: 15471865]

Dorwart MR, Shcheynikov N, Wang Y, Stippec S, Muallem S. SLC26A9 is a Cl channel regulated by the WNK kinases. J Physiol 2007;584:333–45. [PubMed: 17673510]

Everett LA, Glaser B, Beck JC, Idol JR, Buchs A, Heyman M, Adawi F, Hazani E, Nassir E, Baxevanis AD, Sheffield VC, Green ED. Pendred syndrome is caused by mutations in a putative sulphate transporter gene (PDS). Nat Genet 1997;17:411–22. [PubMed: 9398842]

Everett LA, Green ED. A family of mammalian anion transporters and their involvement in human genetic diseases. Hum Mol Genet 1999;8:1883–91. [PubMed: 10469841]

Greeley T, Shumaker H, Wang Z, Schweinfest CW, Soleimani M. Downregulated in adenoma and putative anion transporter are regulated by CFTR in cultured pancreatic duct cells. Am J Physiol Gastrointest Liver Physiol 2001;281:G1301–8. [PubMed: 11668039]

Grichtchenko II II, Choi II, Zhong X, Bray-Ward P, Russell JM, Boron WF. Cloning, characterization and chromosomal mapping of a human electroneutral Na+-driven Cl-HCO_3 exchanger. J Biol Chem 2001;276:8358–8363. [PubMed: 11133997]

Haila S, Hastbacka J, Bohling T, Karjalainen-Lindsberg ML, Kere J, Saarialho-Kere U. Slc26a2 (diastrophic dysplasia sulfate transporter) is expressed in developing and mature cartilage but also in other tissues and cell types. J Histochem Cytochem 2001;49:973–82. [PubMed: 11457925]

Haila S, Saarialho-Kere U, Karjalainen-Lindsberg ML, Lohi H, Airola K, Holmberg C, Hastbacka J, Kere J, Hoglund P. The congenital chloride diarrhea gene is expressed in seminal vesicle, sweat gland,

inflammatory colon epithelium, and in some dysplastic colon cells. Histochem Cell Biol 2000;113:279–86. [PubMed: 10857479]

Hastbacka J, de la Chapelle A, Kaitila I, Sistonen P, Weaver A, Lander E. Linkage disequilibrium mapping in isolated founder populations: diastrophic dysplasia in Finland. Nat Genet 1992;2:204–11. [PubMed: 1345170]

Hastbacka J, Superti-Furga A, Wilcox WR, Rimoin DL, Cohn DH, Lander ES. Sulfate transport in chondrodysplasia. Ann N Y Acad Sci 1996;785:131–6. [PubMed: 8702119]

Hoglund P, Haila S, Scherer SW, Tsui LC, Green ED, Weissenbach J, Holmberg C, de la Chapelle A, Kere J. Positional candidate genes for congenital chloride diarrhea suggested by high-resolution physical mapping in chromosome region 7q31. Genome Res 1996;6:202–10. [PubMed: 8963897]

Ip YK, Chew SF, Randall DJ. Five tropical air-breathing fishes, six different strategies to defend against ammonia toxicity on land. Physiol Biochem Zool 2004;77:768–82. [PubMed: 15547795]

Karniski LP, Lotscher M, Fucentese M, Hilfiker H, Biber J, Murer H. Immunolocalization of sat-1 sulfate/oxalate/bicarbonate anion exchanger in the rat kidney. Am J Physiol 1998;275:F79–87. [PubMed: 9689008]

Kato A, Chang MH, Kurita Y, Nakada T, Hirose S, Romero MF. Functional Characterization of Pufferfish Slc26a6A and Slc26a6B. Faseb J 2008;22

Kim KH, Shcheynikov N, Wang Y, Muallem S. SLC26A7 Is a Cl^- Channel Regulated by Intracellular pH. J Biol Chem 2005;280:6463–70. [PubMed: 15591059]

Knauf F, Yang CL, Thomson RB, Mentone SA, Giebisch G, Aronson PS. Identification of a chloride-formate exchanger expressed on the brush border membrane of renal proximal tubule cells. Proc Natl Acad Sci U S A 2001;98:9425–30. [PubMed: 11459928]

Ko SB, Shcheynikov N, Choi JY, Luo X, Ishibashi K, Thomas PJ, Kim JY, Kim KH, Lee MG, Naruse S, Muallem S. A molecular mechanism for aberrant CFTR-dependent HCO_3^- transport in cystic fibrosis. Embo J 2002;21:5662–72. [PubMed: 12411484]

Ko SB, Zeng W, Dorwart MR, Luo X, Kim KH, Millen L, Goto H, Naruse S, Soyombo A, Thomas PJ, Muallem S. Gating of CFTR by the STAS domain of SLC26 transporters. Nat Cell Biol 2004;6:343–50. [PubMed: 15048129]

Kurita Y, Nakada T, Kato A, Mistry AC, Chang M-H, Romero MF, Hirose S. Identification of intestinal bicarbonate transporters involved in formation of carbonate precipitates to stimulate water absorption in marine teleost fish. Am J Physiol - Comp & Reg Physiol 2008;284:R1402–12.

Liman ER, Tytgat J, Hess P. Subunit stoichiometry of a mammalian K+ channel determined by construction of multimeric cDNAs. Neuron 1992;9:861–71. [PubMed: 1419000]

Lohi H, Kujala M, Kerkela E, Saarialho-Kere U, Kestila M, Kere J. Mapping of five new putative anion transporter genes in human and characterization of SLC26A6, a candidate gene for pancreatic anion exchanger. Genomics 2000;70:102–12. [PubMed: 11087667]

Lohi H, Kujala M, Makela S, Lehtonen E, Kestila M, Saarialho-Kere U, Markovich D, Kere J. Functional characterization of three novel tissue-specific anion exchangers SLC26A7, -A8, and -A9. J Biol Chem 2002;277:14246–54. [PubMed: 11834742]

Mansfield TA, Simon DB, Farfel Z, Bia M, Tucci JR, Lebel M, Gutkin M, Vialettes B, Christofilis MA, Kauppinen-Makelin R, Mayan H, Risch N, Lifton RP. Multilocus linkage of familial hyperkalaemia and hypertension, pseudohypoaldosteronism type II, to chromosomes 1q31-42 & 17p11-q21. Nat Genet 1997;16:202–5. [PubMed: 9171836]

Moseley RH, Hoglund P, Wu GD, Silberg DG, Haila S, de la Chapelle A, Holmberg C, Kere J. Downregulated in adenoma gene encodes a chloride transporter defective in congenital chloride diarrhea. Am J Physiol 1999;276:G185–92. [PubMed: 9886994]

Mount DB, Baekgaard A, Hall AE, Plata C, Xu J, Beier DR, Gamba G, Hebert SC. Isoforms of the Na-K-2Cl cotransporter in murine TAL I. Molecular characterization and intrarenal localization. Am J Physiol 1999;276:F347–58. [PubMed: 10070158]

Mount DB, Romero MF. The SLC26 gene family of multifunctional anion exchangers. Pflügers Arch 2004;447:710–21.

Petrovic S, Ju X, Barone S, Seidler U, Alper SL, Lohi H, Kere J, Soleimani M. Identification of a basolateral Cl^-/HCO_3^- exchanger specific to gastric parietal cells. Am J Physiol Gastrointest Liver Physiol 2003;284:G1093–103. [PubMed: 12736153]

Picollo A, Pusch M. Chloride/proton antiporter activity of mammalian CLC proteins ClC-4 and ClC-5. Nature 2005;436:420–3. [PubMed: 16034421]

Plata C, Sussman CR, Sindic A, Liang JO, Mount DB, Josephs ZM, Chang MH, Romero MF. A novel electroneutral sodium monocarboxylate transport (SMCTn) is present in zebrafish: A comparison to the electrogenic SMCT (SMCTe/Slc5a8). J Biol Chem 2007;282:11996–2009. [PubMed: 17255103]

Romero MF, Chang M-H, Plata C, Zandi-Nejad K, Broumand V, Sussman CR, Mount DB. "Physiology of electrogenic SLC26 paralogs" In - Epithelial Anion Transport in Health and Disease: the role of the SLC26 transporters family. Novartis Foundation Symposium 2006;273:126–147. [PubMed: 17120765]

Romero MF, Fong P, Berger UV, Hediger MA, Boron WF. Cloning and functional expression of rNBC, an electrogenic Na^+-HCO_3^- cotransporter from rat kidney. Am J Physiol 1998;274:F425–32. [PubMed: 9486238]

Romero MF, Hediger MA, Boulpaep EL, Boron WF. Expression cloning and characterization of a renal electrogenic $Na^{+/}HCO_3^-$ cotransporter. Nature 1997;387:409–13. [PubMed: 9163427]

Romero MF, Henry D, Nelson S, Harte PJ, Dillon AK, Sciortino CM. Cloning and characterization of a Na^+ driven anion exchanger (NDAE1): a new bicarbonate transporter. J Biol Chem 2000;275:24552–24559. [PubMed: 10827195]

Satoh H, Susaki M, Shukunami C, Iyama K, Negoro T, Hiraki Y. Functional analysis of diastrophic dysplasia sulfate transporter. Its involvement in growth regulation of chondrocytes mediated by sulfated proteoglycans. J Biol Chem 1998;273:12307–15. [PubMed: 9575183]

Scheel O, Zdebik AA, Lourdel S, Jentsch TJ. Voltage-dependent electrogenic chloride/proton exchange by endosomal CLC proteins. Nature 2005;436:424–7. [PubMed: 16034422]

Schmitt BM, Biemesderfer D, Boulpaep EL, Romero MF, Boron WF. Immunolocalization of the electrogenic Na^+/ HCO_3^- cotransporter in mammalian and amphibian kidney. Am J Physiol 1999;276:F27–36. [PubMed: 9887077]

Schweinfest CW, Henderson KW, Suster S, Kondoh N, Papas TS. Identification of a colon mucosa gene that is down-regulated in colon adenomas and adenocarcinomas. Proc Natl Acad Sci U S A 1993;90:4166–70. [PubMed: 7683425]

Sciortino CM, Fletcher BR, Shrode LD, Harte PJ, Romero MF. Localization of Endogenous and Recombinant Na^+-driven Anion Exchanger Protein, NDAE1, from Drosophila melanogaster. Am J Physiol Cell Physiol 2001;281:C449–63. [PubMed: 11443044]

Sciortino CM, Romero MF. Cation and voltage dependence of rat kidney, electrogenic $Na^{+/}HCO_3^-$ cotransporter, rkNBC, expressed *in* oocy*tes*. Am J Physiol 1999;277:F611–623. [PubMed: 10516286]

Scott DA, Karniski LP. Human pendrin expressed in Xenopus laevis oocytes mediates chloride/formate exchange. Am J Physiol Cell Physiol 2000;278:C207–C211. [PubMed: 10644529]

Scott DA, Wang R, Kreman TM, Sheffield VC, Karniski LP. The Pendred syndrome gene encodes a chloride-iodide transport protein. Nat Genet 1999;21:440–3. [PubMed: 10192399]

Shcheynikov N, Wang Y, Park M, Ko SB, Dorwart M, Naruse S, Thomas PJ, Muallem S. Coupling Modes and Stoichiometry of Cl-/HCO3- Exchange by slc26a3 and slc26a6. J Gen Physiol 2006;127:511–24. [PubMed: 16606687]

Soleimani M, Greeley T, Petrovic S, Wang Z, Amlal H, Kopp P, Burnham CE. Pendrin: an apical Cl^-/ OH^-/HCO_3^- exchanger in the kidney cortex. Am J Physiol Renal Physiol 2001;280:F356–64. [PubMed: 11208611]

Wang S, Yue H, Derin RB, Guggino WB, Li M. Accessory protein facilitated CFTR-CFTR interaction, a molecular mechanism to potentiate the chloride channel activity. Cell 2000;103:169–79. [PubMed: 11051556]

Wheat VJ, Shumaker H, Burnham C, Shull GE, Yankaskas JR, Soleimani M. CFTR induces the expression of DRA along with Cl(-)/HCO(3)(-) exchange activity in tracheal epithelial cells. Am J Physiol Cell Physiol 2000;279:C62–71. [PubMed: 10898717]

Xie Q, Welch R, Mercado A, Romero MF, Mount DB. Molecular and functional characterization of the Slc26A6 anion exchanger, functional comparison to Slc26a1. Am J Physiol Renal Physiol 2002a; 283:F826–838. [PubMed: 12217875]

Xie Q, Welch R, Song L, Romero MF, Mount DB. Cloning of multiple novel members of the SLC26 gene family of anion exchangers. FASEB J 2002b;16:a807.

Xu J, Henriksnas J, Barone S, Witte D, Shull GE, Forte JG, Holm L, Soleimani M. SLC26A9 is expressed in gastric surface epithelial cells, mediates Cl^-/HCO_3^- exchange and is inhibited by NH_4^+ Am J Physiol Cell Physiol 2005;289:C493–505. [PubMed: 15800055]

Xu J, Song P, Miller ML, Borgese F, Barone S, Riederer B, Wang Z, Alper SL, Forte JG, Shull GE, Ehrenfeld J, Seidler U, Soleimani M. Deletion of the chloride transporter Slc26a9 causes loss of tubulovesicles in parietal cells and impairs acid secretion in the stomach. Proc Natl Acad Sci U S A 2008;105:17955–17960. [PubMed: 19004773]

Zheng J, Shen W, He DZ, Long KB, Madison LD, Dallos P. Prestin is the motor protein of cochlear outer hair cells. Nature 2000;405:149–55. [PubMed: 10821263]

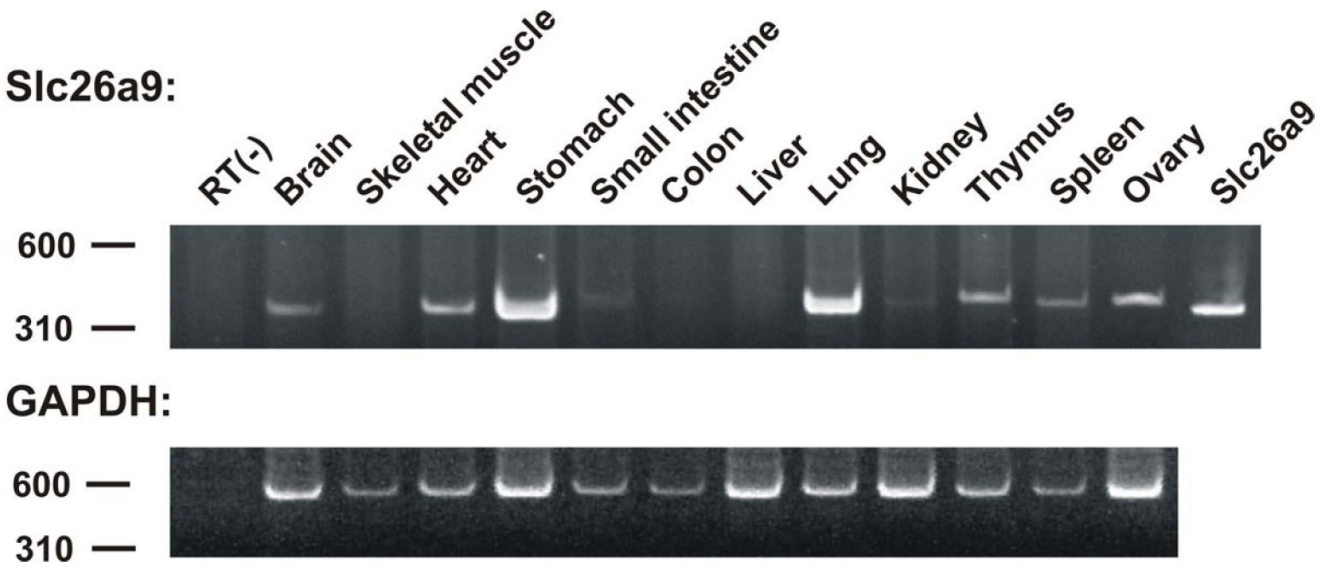

Fig 1. Slc29a9 mRNA distribution

RT-PCR of mouse tissues showing the wider distribution of Slc26a9 mRNA (brain, heart, small intestine, kidney, thymus, spleen and ovary).

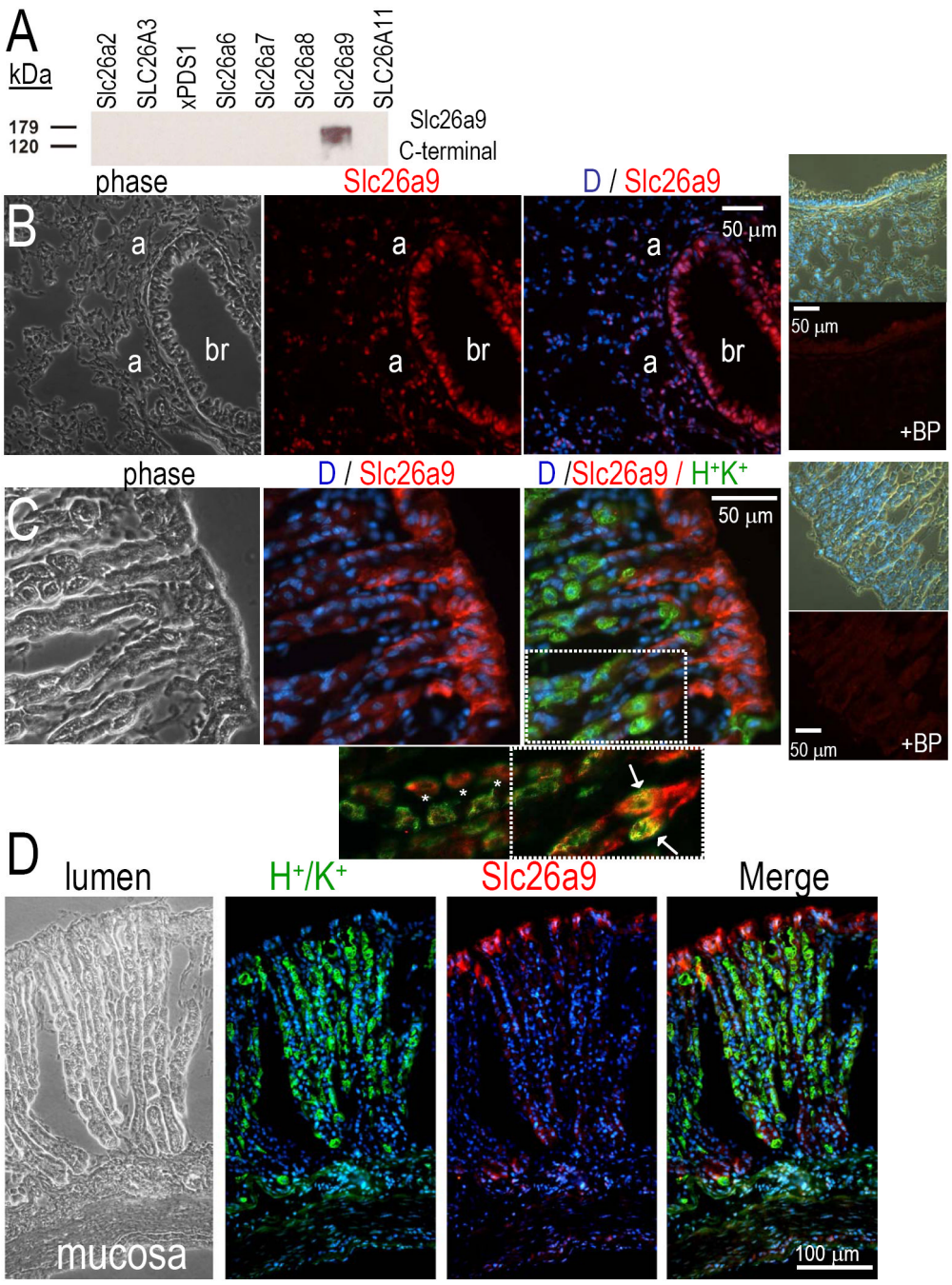

Fig 2. Immunolocalization of Slc26a9 protein in lung and stomach

Panel A, Slc26 proteins were expressed in *Xenopus* oocytes by injecting cRNA. Rabbit polyclonal antibodies for Slc26a9 were used to probe Western blots of oocyte membranes. Panel B shows mouse lung tissue: Slc26a9 staining (cy3, red) with DAPI (blue, nuclei). Right smaller panels show both phase and fluorescence of mouse lung in the presence of the Slc26a9 blocking peptide (BP). Panel C shows mouse stomach: co-labeling of Slc26a9 (red), HK-pump (green) and DAPI (blue, nuclei). Right smaller panels show both phase and fluorescence of mouse stomach in the presence of the Slc26a9 BP. Panel C (inset) shows a magnification and extension of the merged view. Removal of the Dapi stain and enhanced red-contrast shows that there is both colocalization of Slc26a9 and the H^+/K^+ pump (arrows and yellow) as well as

adjacent staining (*) in the central cells of the crypt. Panel D is a montage of the complete gastric crypt-villus axis: Slc26a9 (red), HK-pump (green), DAPI (blue), Merge (red, green, blue fluorescent overlay).

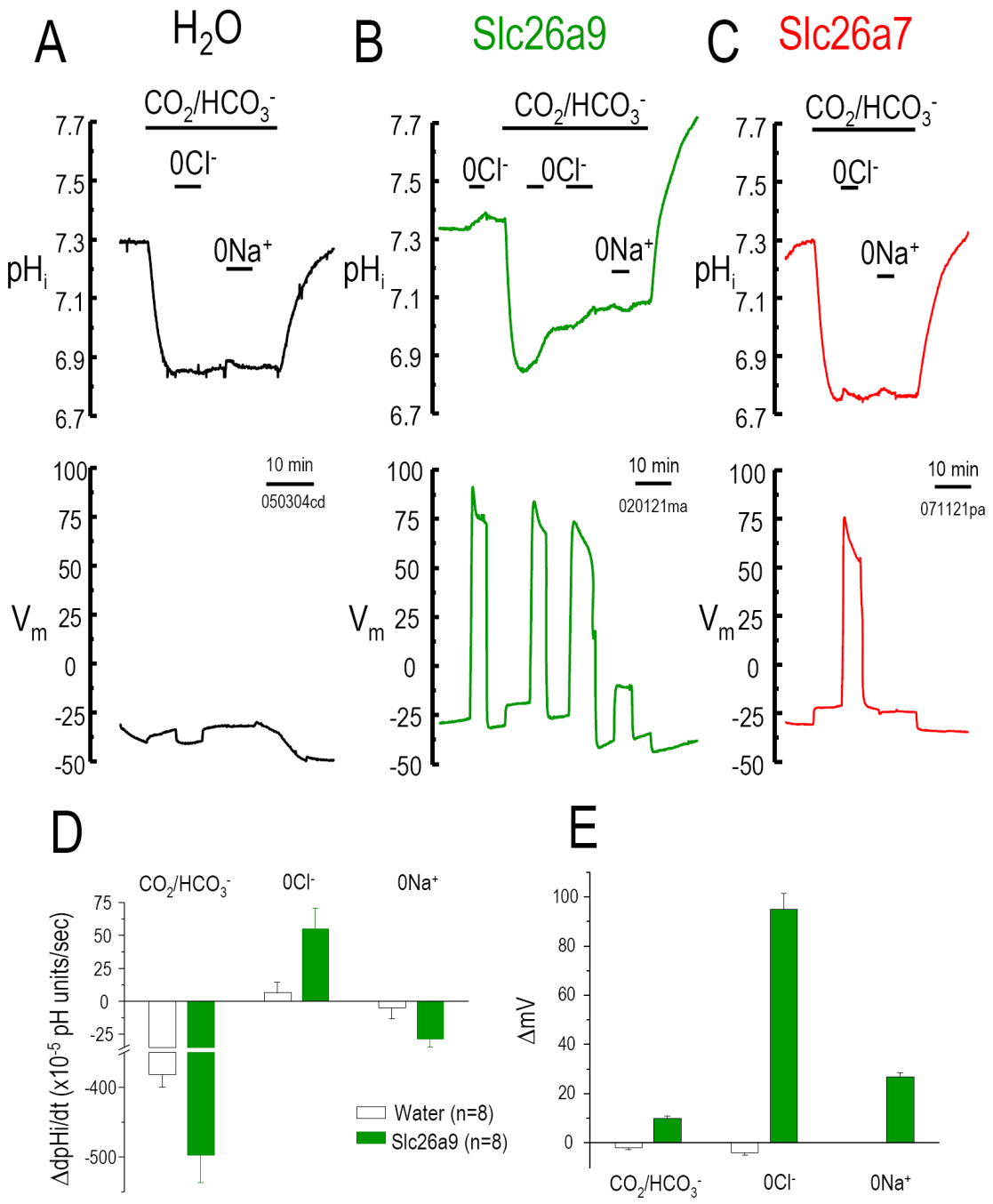

Fig 3. Cl^--HCO_3^- exchange activity

Intracellular pH (pH_i) and membrane potential (V_m) changes of water injected Xenopus oocyte (A) and oocytes expressing Slc26a9 (B) or Slc26a7 (C) are measured using microelectrodes (see **Methods**). Bath Cl^- removal ($0Cl^-$, gluconate replacement) in the presence of 5% CO_2/ 33 mM HCO_3^- (pH 7.5) will increase pH_i as Cl^- moves out of the oocyte in exchange for HCO_3^- (moving into oocyte). Na^+ removal (in CO_2/HCO_3^-) is an indication of Na^+/HCO_3^- cotransporter activity (Na^+ and HCO_3^- moving out of the oocyte together). $0Cl^-$ elicits a pHi increase (base loading) in Slc26a9 (B) cells but not Slc26a7 (C). $0Cl^-$ also elicits a Vm increase for both Slc26a9 and Slc26a7. Averaged pHi change rates (10^{-5} pH units/sec) and membrane

potential changes (ΔmV) due to addition of CO_2/HCO_3^-, Cl^- removal, and Na^+ removal are shown in D and E, respectively.

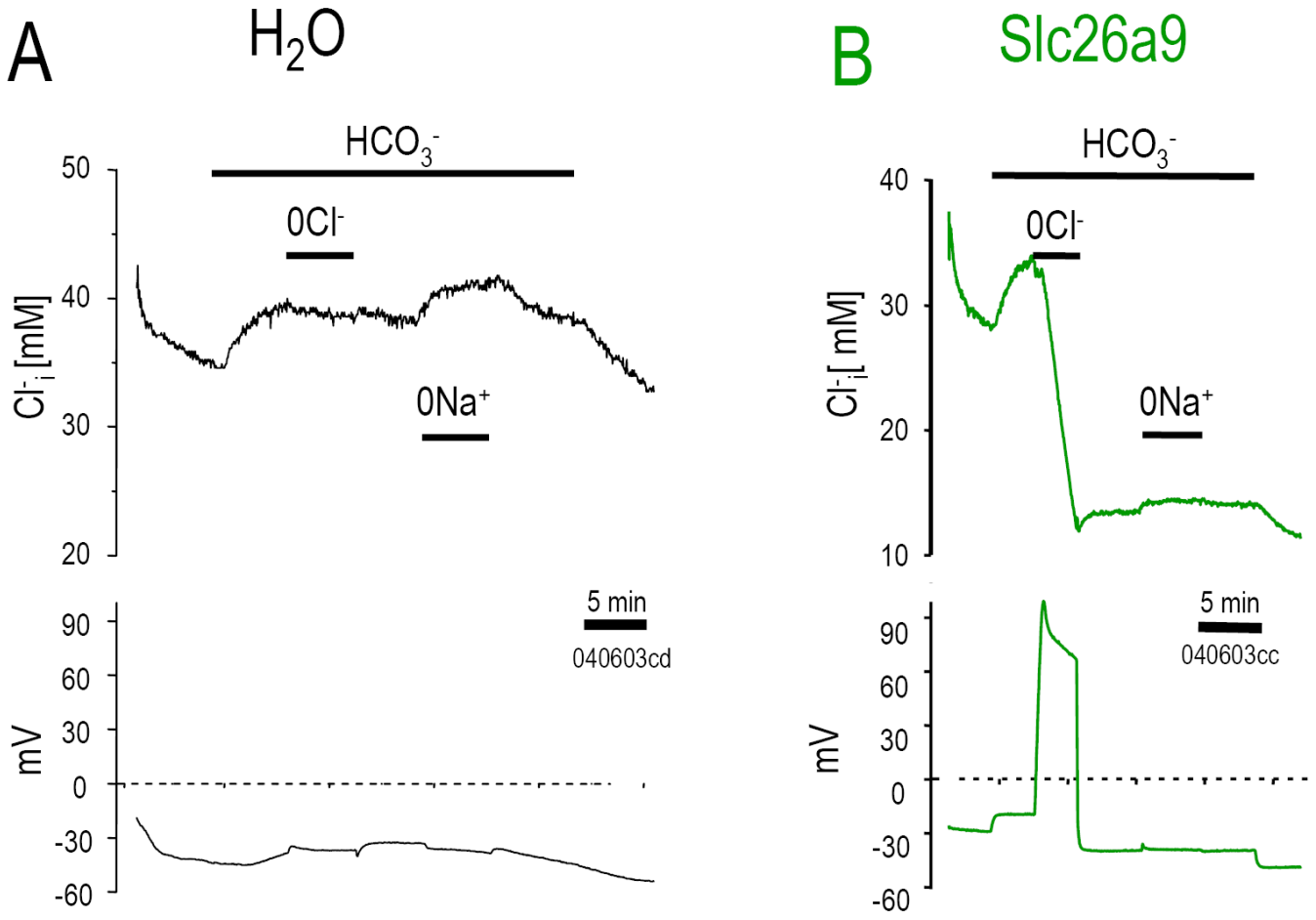

Fig 4. Cl^- transport

Oocytes were perfused while monitoring $[Cl^-]_i$ (upper panels) and Vm (lower panels) for water (A), and Slc26a9 (B). Cl^- was replaced with gluconate and Na^+ was replaced with NMDG. Removal of Cl^- from extracellular 33 mM HCO_3^- solution resulting in dramatic fall in $[Cl^-]_i$ and simultaneously depolarizing the cell depicts multiple Cl^- exchange for one HCO_3^- transport of Slc26a9.

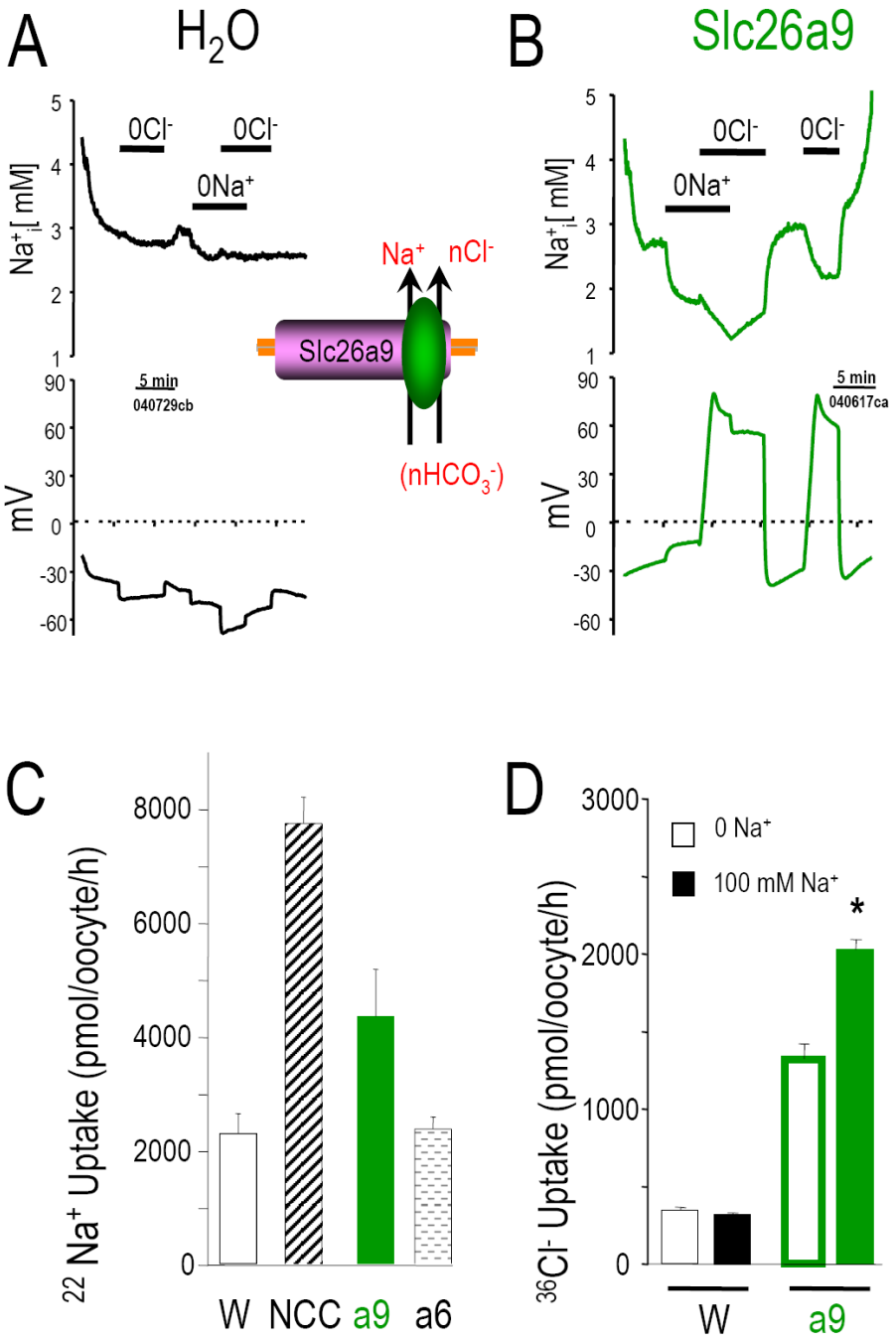

Fig 5. Na^+ transport

Oocytes were perfused while monitoring $[Na^+]_i$ (upper panels) and V_m (lower panels) for water (A), and Slc26a9 (B). Cl^- was replaced with gluconate and Na^+ was replaced with NMDG. Removal of Na^+ from extracellular solution resulting in a slight depolarization of the cell in addition to a moderate decrease of $[Na^+]_i$ in Slc26a9. These two reversible transport modes are not observed in H_2O injected oocyte under the same solution maneuver. (C), Robust and moderate $^{22}Na^+$ uptake was observed in Na^+-Cl^- cotransporter (NCC) Slc26a9, respectively, but not in Slc26a6. This data again strengthened our hypothesis that Slc26a9 can transport Na^+ directly. (D), Slc26a9 mediated $^{36}Cl^-$ uptake is augmented by the presence of Na^+ in the uptake media.

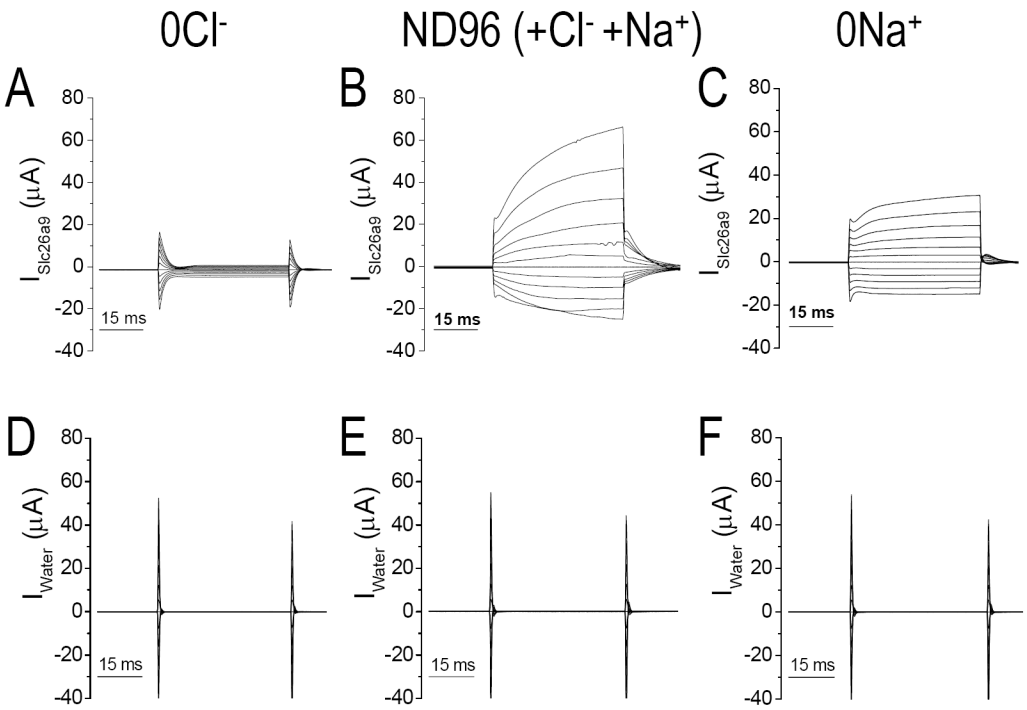

Fig 6. Whole cell currents of Slc26a9

Slc26a9- (A-C) and water injected control (D-F) oocytes are voltage clamped at -60 mV and in various extracellular solution, 40 ms I-V protocols were executed from V_h of −160 mV to +60 mV in 20 mV step then filtered at 2-5 kHz and recorded at 10Hz. ND96 (B) has extracellular Cl^- concentration of 104 mM and 96 mM Na^+. Cl^- was replaced with gluconate and Na^+ was replaced with NMDG.

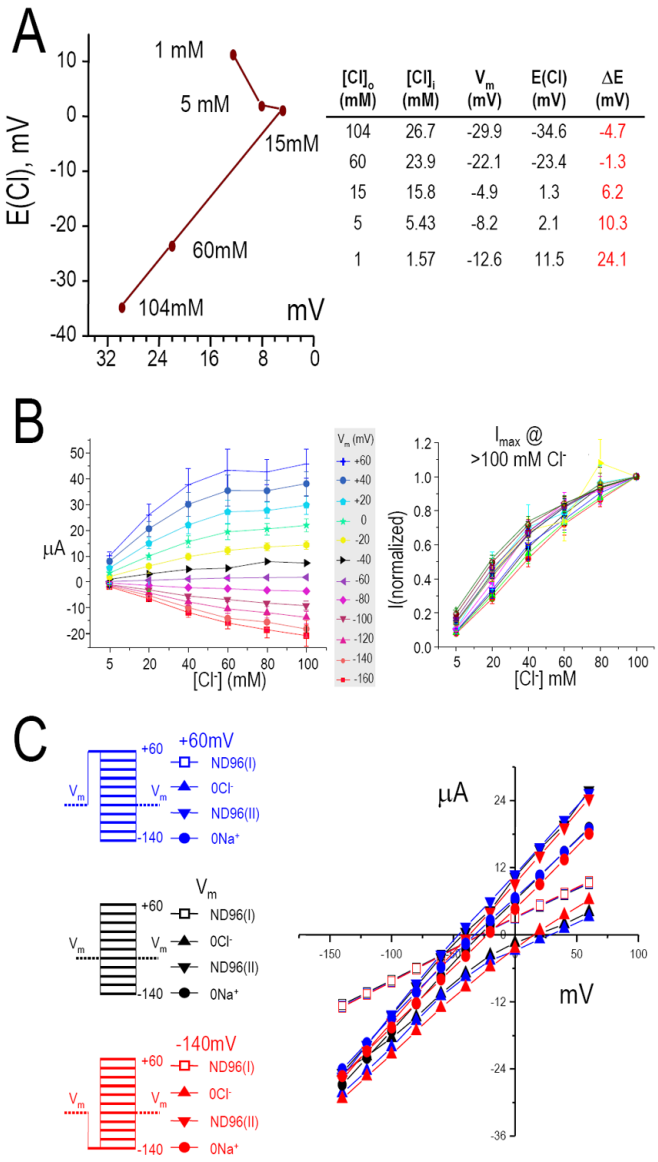

Fig 7. Anion conductance of Slc26a9

(A) intracellular Cl^- concentration $[Cl^-]_i$ and V_m were measured simultaneously while the extracellular Cl^- concentrations ($[Cl^-]_o$) were varied from 1 to 104 mM. There is a linear relationship between the equilibrium potential (E(Cl)) and $[Cl^-]_o$ from 15-104 mM Cl^-. (B), Voltage clamp steps of Slc26a9 currents elicited by various extracellular Cl^- concentrations from 0 to 104 mM (left). Data shown are averaged values from 6 oocytes and color coded for each holding voltages. Currents are normalized to values measured at 104 mM extracellular Cl^- at each respective holding voltage (right). These data also indicate that the I(max) for Cl^- occurs at greater than 104 mM. (**C**), Comparing the IV relationships for Slc26a9 at +60 mV (blue), resting V_m (black) or -140 mV (red) pre-pulse before the pulse protocol were executed while extracellular Cl^- or Na^+ were present (open squares, ND96(I) and closed inverted triangles, ND96(II)) or replaced ($0Cl^-$, filled triangles; $0Na^+$, filled circles). The IV relationships for Slc26a9 are not pre-pulse dependent

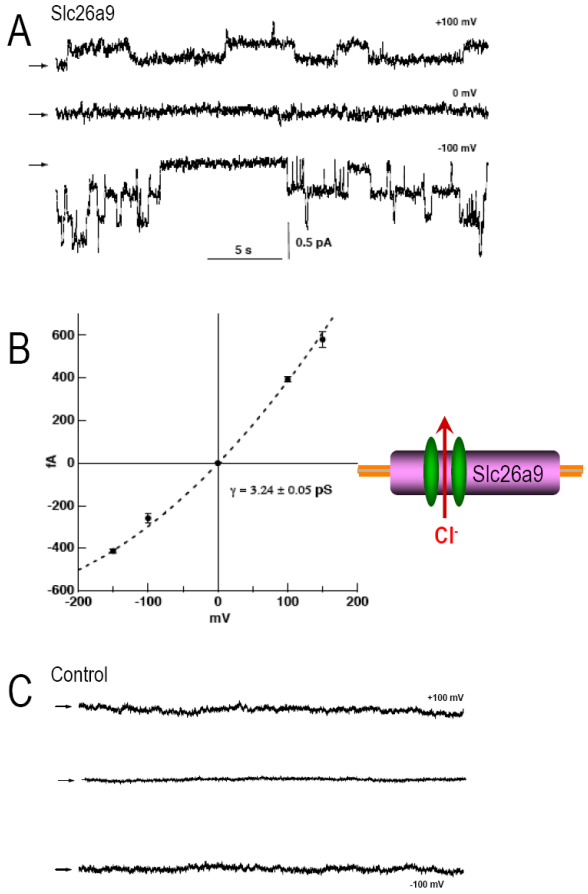

Fig 8. Slc26a9 displays single channel events

(A) Slc26a9 Cl^- channels in an inside-out patch with symmetrical (140 mM) NMDG-Chloride at various pipette potentials (+100, 0, -100 mV). Representative recordings are from CHO cells transiently expressing Slc26a9. Arrows indicate the baseline levels. (B) Single channel current-voltage relationships of Slc26a9 channels. Data points are mean ± sem of 3-6 experiments at each voltage. Dotted line is mean slope conductance fitted to the data points. (C) Recordings of non-transfected CHO cells at various pipette potentials (+100, 0, -100 mV).

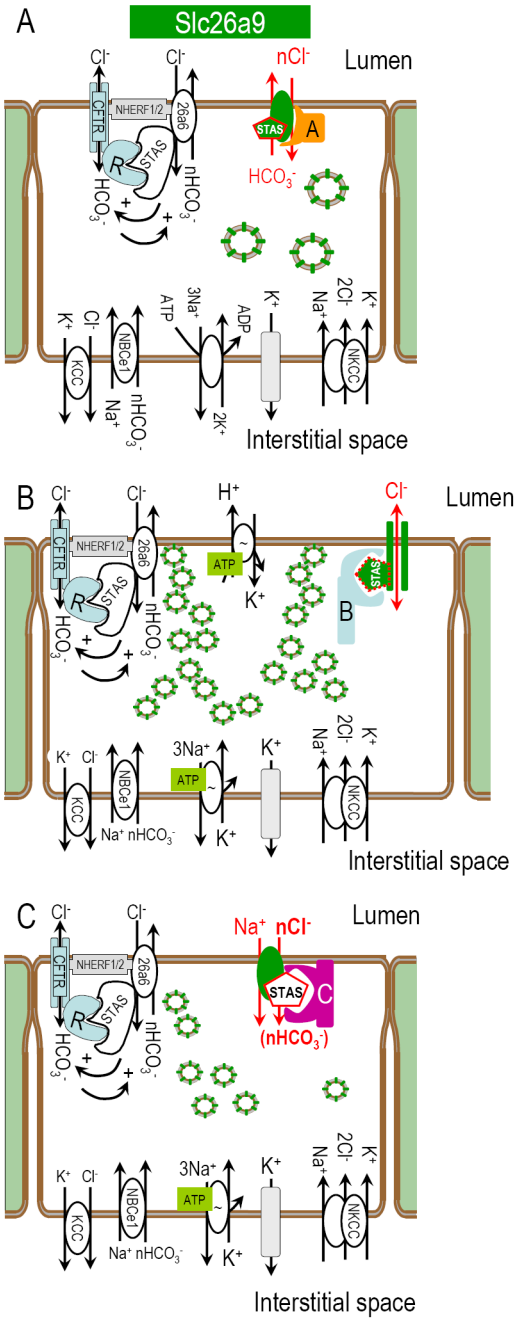

Fig 9. Model of Slc26a9 function in stomach and lung

Epithelial cell models incorporating Slc26a9 at the apical membrane as a putative player in transepithelial NaCl absorption and H^+ secretion. Panel **A** depicts an epithelial cell which is both absorbing Cl^- and secreting HCO_3^-. Slc26a9 is also indicated in intracellular vesicles to be consistent with the intracellular staining observed. These putative vesicles could be recruited to the plasma membrane as a mechanism for controlling the amount of Slc26a9 plasma membrane function. Panel **B** depicts one potential model of H^+ in the gastric parietal cell (note extensive vesicles which would form the tubular canaliculi upon stimulation). While the parietal cell model shows Slc26a9 as a Cl^- channel, it is also possible to accomplish the H^+ secretion with Slc26a9 as an electrogenic Cl^--HCO_3^- exchanger (**A**). Panel **C** illustrates an

epithelial cell in which Slc26a9 plays the role of a $Na^+/\underline{n}Anion^-$ cotransporter. These panels also depict putative interacting proteins that would "switch" the physiological mode of Slc26a9 (currently hypothetical).

Table I

PCR primers used

Primer Name	Primer Sequence	Use
Human SLC26A9 forward	5′-TAgACAgAgCCgCATACTCCCTTACCCTCTTC-3′	Cloning SLC26A9
Human SLC26A9 reverse	5′-gATgTgCTTgCTgACAgCAgTggTggTTTgg-3′	Cloning SLC26A9
Mouse Slc26a9 forward	5′-CAAAgCTTgTCAATgTCCCAgACATgAACCAgC	Cloning mSlc26a9
Mouse Slc26a9 reverse	5′-CCACTgTCCACACTAgAgTCTgAAgTgCTggACAgC	Cloning mSlc26a9
Slc26a9 forward	5′-GCTGAGGCTCACATATCCTAC-3′	RT-PCR
Slc26a9 reverse	5′-AGAGGACTGCATCGTGGATG-3′	RT-PCR
GAPDH forward	5′-TCACCATCTTCCAGGAGCG-3′	RT-PCR
GAPDH reverse	5′-CTGCTTCACCACCTTCTTGA-3′	RT-PCR